frontiers in Earth Science

ORIGINAL RESEARCH
published: 23 March 2022
doi: 10.3389/feart.2022.830984

Calcium Carbonate Dissolution Triggered by High Productivity During the Last Glacial–Interglacial Interval in the Deep Western South Atlantic

Jaime Y. Suárez-Ibarra[1,2], Cristiane F. Frozza[1], Pâmela L. Palhano[1], Sandro M. Petró[3], Manuel F. G. Weinkauf[2] and Maria A. G. Pivel[4]*

[1]Programa de Pós-Graduação Em Geociências, Instituto de Geociências, Universidade Federal Do Rio Grande do Sul, Porto Alegre, Brazil, [2]Ústav Geologie a Paleontologie, Přírodovědecká Fakulta, Univerzita Karlova, Prague, Czech Republic, [3]itt OCEANEON, Instituto Tecnológico de Paleoceanografia e Mudanças Climáticas, Universidade Do Vale Do Rio Dos Sinos, São Leopoldo, Brazil, [4]Instituto de Geociências, Universidade Federal do Rio Grande do Sul, Porto Alegre, Brazil

OPEN ACCESS

Edited by:
Jacek Raddatz,
Goethe University Frankfurt, Germany

Reviewed by:
Selvaraj Kandasamy,
Xiamen University, China
Patrick Grunert,
University of Cologne, Germany

***Correspondence:**
Jaime Y. Suárez-Ibarra
jysuarezibarra@gmail.com
suarezij@natur.cuni.cz

Specialty section:
This article was submitted to Quaternary Science, Geomorphology and Paleoenvironment, a section of the journal Frontiers in Earth Science

Received: *07 December 2021*
Accepted: *17 February 2022*
Published: *23 March 2022*

Citation:
Suárez-Ibarra JY, Frozza CF, Palhano PL, Petró SM, Weinkauf MFG and Pivel MAG (2022) Calcium Carbonate Dissolution Triggered by High Productivity During the Last Glacial–Interglacial Interval in the Deep Western South Atlantic. Front. Earth Sci. 10:830984. doi: 10.3389/feart.2022.830984

Studies reconstructing surface paleoproductivity and benthic environmental conditions allow us to measure the effectiveness of the biological pump, an important mechanism in the global climate system. In order to assess surface productivity changes and their effect on the seafloor, we studied the sediment core SAT-048A, spanning 43–5 ka, recovered from the continental slope (1,542 m water depth) of the southernmost Brazilian continental margin, deep western South Atlantic. We assessed the sea surface productivity, the organic matter flux to the seafloor, and calcite dissolution effects, based on micropaleontological (benthic and planktonic foraminifers, ostracods), geochemical (benthic $\delta^{13}C$ isotopes), and sedimentological data (carbonate and bulk sand content). Superimposed on the induced changes related to the last glacial–interglacial transition, the reconstruction indicates a significant and positive correlation between the paleoproductivity proxies and the summer insolation. From the reconstructed data, it was possible to identify high (low) surface productivity, high (low) organic matter flux to the seafloor, and high (low) dissolution rates of planktonic Foraminifera tests during the glacial (postglacial). Furthermore, within the glacial, enhanced productivity was associated with higher insolation values, explained by increased northeasterly summer winds that promoted meandering and upwelling of the nutrient-rich South Atlantic Central Water. Statistical analyses support the idea that productivity is the main cause for seafloor calcium carbonate dissolution, as opposed to changes in the Atlantic Meridional Overturning Circulation (at least for the 25–4 ka period). Further efforts must be invested in the comprehension and quantification of the total organic matter and biogenic carbonate burial during time intervals with an enhanced biological pump, aiming to better understand their individual roles.

Keywords: planktonic Foraminifera, stable isotopes, Atlantic meridional overturning circulation, upper circumpolar deep water, North Atlantic deep water

INTRODUCTION

The oceanic biological pump is a primary mechanism to exchange CO_2 between the atmosphere and the oceans, and is therefore critically important for the acidity of the sea water and associated carbonate dissolution (Riebesell, 2004). An intensified biological pump in the oceans leads to an increase of exported biogenic carbon and carbonate burial in the sediments (Brummer and van Eijden, 1992). Since planktonic Foraminifera are important contributors to the pelagic calcium carbonate flux (Milliman et al., 1999; Schiebel, 2002; Kučera, 2007) they represent an important component of the global climate system through their role in the oceanic carbon and carbonate pump. The connection between strong changes in the oceanic biological pump and calcite dissolution is difficult to study in modern oceans, as sample areas with sufficient differences in bioproductivity also differ in several other environmental factors, thus confounding the results. In contrast, Pleistocene climate scenarios offer the possibility to investigate a relatively stable ecosystem under intensely changing bioproductivity scenarios.

The Late Quaternary climate is characterized by orbit-related glacial–interglacial fluctuations (EPICA Community Members, 2004; Jouzel et al., 2007) associated with CO_2 variations (Petit et al., 1999; Shakun et al., 2012). Nevertheless, the orbital forcing alone is not strong enough to induce the observed temperature changes and, thus, feedback mechanisms in the Earth's climate system are expected to have amplified (or reduced) the primary signal (Lorius et al., 1990; Shackleton, 2000). The oceanic carbonate pump system is critically influenced by changes in bioproductivity. High biological surface productivity can boost population densities and biomass of benthic communities, increasing the respiration processes and leading to the remineralization of higher percentages of organic matter (OM), resulting in the release of CO_2 and a reduction of the biologic carbon burial (Cronin et al., 1999; Hales, 2003). Besides, higher CO_2 release at the seafloor can lead to increased dissolution of biogenic carbonate, (e.g., planktonic Foraminifera tests; Schiebel, 2002). Therefore, an enhanced biological pump can have an unexpected effect, both decreasing the OM burial and dissolving biogenic carbonates, inhibiting higher quantities of C to be stored in the seafloor sediments (e.g., Zamelczyk et al., 2012; Naik et al., 2014).

Supra-lysoclinal pelagic carbonate dissolution has been described from the western South Atlantic in the past, being related to changes in bottom water masses (Petró et al., 2018a; Petró and Burone, 2018; Petró et al., 2021). Nevertheless, the relation between calcium carbonate dissolution and sea surface productivity has not yet been approached in the studied area. In this paper, we 1) reconstruct past changes in primary and export productivity during the last glacial–interglacial interval, 2) determine mechanisms that triggered calcium carbonate dissolution, and 3) investigate the role of productivity changes on carbonate corrosion from a core retrieved above the lysocline.

Oceanographic Setting

The studied sediment core was recovered off Santa Marta Cape in the western South Atlantic (**Figure 1A,B**). The proximal portion of the continental shelf of the Pelotas Basin represents a submerged coastal plain (Martins, 1984) that was exposed during the last Pleistocene regression (Marine Isotope Stage 2) and dissected by drainage networks from fluvial systems (Weschenfelder et al., 2014), which contributed to larger nutrient inputs from continental outflows compared to the Holocene.

Surface circulation in the shelf portion of the study area is dominated by the northward flowing Brazil Coastal Current, which carries the Coastal Water (CW), a mixture of oceanic and continental drainage waters. Offshore, the Brazil Current (BC) transports the warm (temperature, $T > 20^{\circ}C$) and salty (salinity, $S > 36$) Tropical Water (TW) southwards within the surface layer. The BC flows along the South American margin slope until it converges with the Malvinas Current (MC), a northward flowing surface current carrying the cold ($T < 15^{\circ}C$) and fresher ($S < 34.2$) Subantarctic Water, forming the Brazil/Malvinas Confluence (BMC) close to 38°S (Gordon and Greengrove, 1986). The BMC forms a large meander, which separates southward of the continental margin (Peterson and Stramma, 1991; Piola and Matano, 2017), and varies seasonally and interannually, moving to the north in austral autumn and winter, and to the south in spring and summer. This variation influences the nutrient distribution along the continental shelf of the Argentinian, Uruguayan, and south Brazilian coasts (Gonzalez-Silvera et al., 2006). Presently, two main continental sources of nutrients and freshwater for the area are the Río de la Plata Estuary (RdlPE) and the Patos-Mirim Lagoon System (PMLS). Although the configuration of continental drainage certainly changed under the varying sea-level conditions of the late Quaternary, they both represent sources of continental drainage and, thus, nutrients to the study area.

The water masses that circulate in the subsurface (**Figure 1C**) immediately below the TW are: the South Atlantic Central Water (SACW), the Antarctic Intermediate Water (AAIW), the Upper Circumpolar Deep Water (UCDW), the North Atlantic Deep Water (NADW), and the Antarctic Bottom Water (AABW) (Reid et al., 1976; Campos et al., 1995; Hogg et al., 1996; Stramma and England, 1999). The NADW promotes the preservation of carbonate, due to its oversaturation with carbonate ion (CO_3^{2-}) when compared to the overlying UCDW and the underlying AABW. Both, the UCDW and AABW, are undersaturated in CO_3^{2-} and, therefore, may lead to the dissolution of carbonate (Frenz et al., 2003). Indeed, Frenz and Henrich (2007) have shown that the depth of the interface between the NADW and the AABW defines the lysocline, below which carbonate dissolution occurs.

MATERIALS AND METHODS

The piston core SAT-048A was collected by *FUGRO Brasil–Serviços Submarinos e Levantamentos Ltda* for the *Agência Nacional do Petróleo* (ANP, Brazilian National Agency of Petroleum, Natural Gas and Biofuels) at 29°11′ S and 47°15′ W at 1,542 m water depth (**Figure 1**). The core, with a total recovery of 315 cm, was sampled at intervals of about 6 cm, for a total of 54

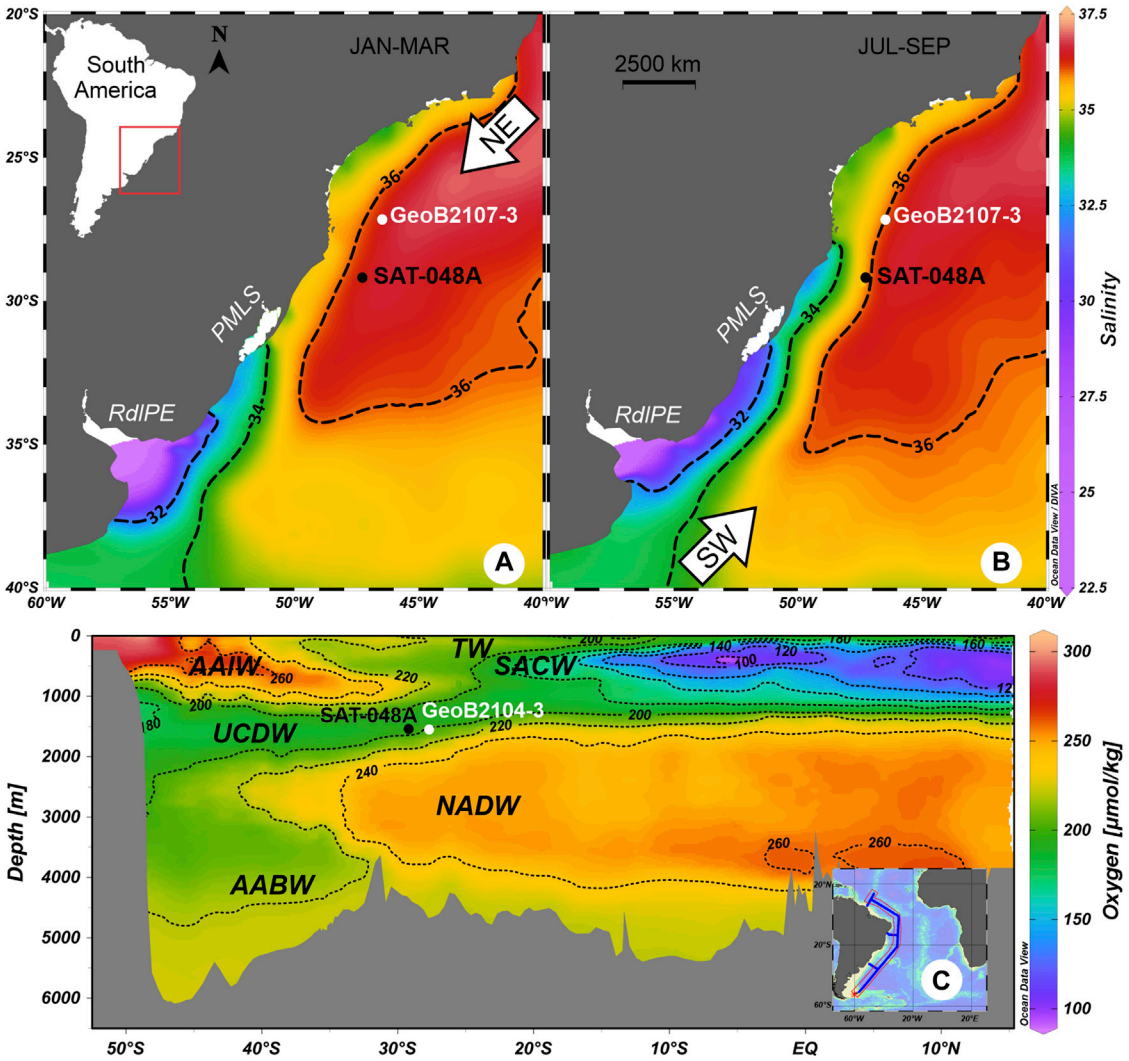

FIGURE 1 | Location of sediment core SAT-048A and other mentioned cores (GeoB2107-3, Gu et al., 2017, Pereira et al., 2018; GeoB2104-3, Howe J. N. W. et al., 2016) in the studied area, in map view **(A,B)** and as latitudinal cross section (C). Seasonal variation of average sea surface salinity (measured on the psu scale) for the months of (a) January–March (austral summer) and (b) July–September (winter) are based on data from the World Ocean Atlas 2013 (WOA13, Zweng et al., 2013). The isohalines 32, 34, and 36 (dashed lines) highlight the northward intrusion of less saline water from the south during winter (b) when compared to summer (a) conditions. This is related to seasonally predominating wind regimes, indicated as white arrows. The present Río de la Plata Estuary (RdlPE) and Patos-Mirim Lagoon System (PMLS) represent important continental nutrient sources in the study area. Dissolved oxygen concentrations (c; µmol/kg) in a transect along the South American continental margin show the South Atlantic water masses that circulate in the region: Tropical Water (TW), South Atlantic Central Water (SACW), Antarctic Intermediate Water (AAIW), Upper Circumpolar Deep Water (UCDW), North Atlantic Deep Water (NADW), and Antarctic Bottom Water (AABW).

samples. The core was missing the top 20 cm and the 196–217 cm interval. Each sample was washed over a 63 µm sieve and oven dried at temperatures below 60°C. The taxonomical identification of the planktonic Foraminifera species, from subsamples of at least 300 specimens larger than 150 µm split with a microsplitter, followed Bé (1967), Bé et al. (1977), Bolli and Saunders (1989), Hemleben et al. (1989), Kemle-von Mücke and Hemleben (1999), Schiebel and Hemleben (2017), and Morard et al. (2019).

We used a revised version of the Frozza et al. (2020) age model, based on the *rbacon* package (Blaauw and Christen, 2011; version 2.4.2) for the R software (R Core Team, 2019). The age model (**Supplementary Material**) used the ten AMS radiocarbon dates presented by Frozza et al. (2020), carried out on monospecific samples of planktonic Foraminifera, and the Laschamp geomagnetic excursion (J. Savian, personal communication, June 5, 2020) as an additional control point.

Past sea surface temperatures (SST) at 100 m water depth (SST_{100m}) were estimated using the modern analogue technique (MAT; Hutson, 1980) in the software PAST (version 4.05; Hammer et al., 2001). The paleo-SST_{100m} were calibrated with a dataset composed of: 1) relative abundances of planktonic Foraminifera of surface sediments from the South Atlantic Ocean extracted from the ForCenS database (Siccha and Kučera, 2017) as training data and 2) modern mean annual

temperature estimates for 100 m below sea level, obtained from the World Ocean Atlas 2013 (Locarnini et al., 2013) and extracted with the software Ocean Data View (Schlitzer, 2020). For the weighting parameter, we used the inverse dissimilarity based on the squared Chord dissimilarity index with a threshold of 0.28 and five analogues.

Sea surface paleo-productivity was assessed from the relative abundances of the species *Globigerinita glutinata* (Conan and Brummer, 2000; Souto et al., 2011) and the ratio between *Globigerina bulloides* and *Globigerinoides ruber* (*albus* and *ruber*) (*G.bull*:*G.rub*; Conan et al., 2002; Toledo et al., 2008). The OM flux to the seafloor, as a response to sea surface productivity, was estimated based on the benthic:planktonic Foraminifera ratio (B:P; Berger and Diester-Haass, 1988; Loubere, 1991; Gooday, 2002). While this parameter was applied on different size fractions in the past, with no clearly defined standard, it was shown that small size fraction differences do not impact analyses considerably (Schönfeld 2012; Weinkauf. 2018). As long as data for benthic and planktonic communities, as in our case, were extracted from the same sieve size fraction. The resulting B:P ratios will be comparable, indeed, being used in the literature (e.g., de Almeida et al., 2022). The ostracod valves abundances (number of valves in the >150 μm fraction per gram of sediment), and the $\delta^{13}C$ record of *Uvigerina* spp. ($\delta^{13}C_{Uvi}$; Mackensen, 2008) were also used to infer the OM flux to the seafloor. Part of these data (relative abundances of *G. bulloides* and *G. ruber*, $\delta^{13}C_{Uvi}$) were previously published by Frozza et al. (2020). For the $\delta^{13}C_{Uvi}$ measurements, approximately seven specimens of the benthic foraminiferal genus *Uvigerina* were selected from the 250 μm sediment fraction from each sample. The geochemical analyses were performed with a Thermo Scientific MAT-253 mass spectrometer, coupled to a Kiel IV carbonate device, by the Laboratory of Stable Isotopes of the University of California–Santa Cruz (SIL-UCSC). All results are expressed in *δ*-notation relative to the Vienna Pee-Dee Belemnite (VPDB) standard.

Dissolution effect proxies for this core were published by Suárez-Ibarra et al. (2021) and were based on the 1) the planktonic Foraminifera fragmentation intensity, which follows Berger (1970)'s fragments and broken shells counting, 2) the bulk sand fraction (%; Berger et al., 1982; Gonzales et al., 2017), 3) the number of whole planktonic Foraminifera tests per Gram of sediment (PF/g, Le and Shackleton, 1992), and 4) the relative $CaCO_3$ content of the sediment. Bulk sand contents were determined using a laser diffraction particle size analyzer Horiba Partica-LA-950 at the Climate Studies Center Centro de Estudo de Geologia Costeira e Oceânica (CECO) of the Universidade Federal do Rio Grande do Sul (UFRGS). The calcium carbonate content for the samples was determined by weight loss after reaction with 10% hydrochloric acid (HCl) at the Calcareous Microfossils Laboratory of the UFRGS.

All statistical analyses were conducted in the software PAST (version 4.05; Hammer et al., 2001). An overall relation between productivity and dissolution proxies was quantified using Spearman rank-order correlation. To objectively define phases of changing conditions through the analyzed time interval, a principal component analysis (PCA) on the correlation matrix including all the correlatable paleo-productivity proxies (PCA_P) and all dissolution proxies (PCA_D), respectively, was carried out. Using the first principal component of PCA_P ($PC1_P$), we objectively defined the borders between the three phases using a piecewise ordinary least-squares regression (OLS; Weinkauf et al., 2013): 1) We subdivided the $PC1_P$ vs age date into three subsets. The age-borders for each subset varied over a range of reasonable values (25.11–31.46 ka for the phase 1–Phase 2 border, 18.274–15.515 ka for the phase 2–Phase 3 border); 2) for each possible combination of phase borders, we calculated three independent OLS regression lines and their associated R^2-value; 3) we calculated the overall fit of the solution as the product of the three individual R^2-values; 4) the best phase border solution was the one that showed the highest overall R^2-value. The relationship between summer insolation and paleo-productivity, represented by the score of $PC1_P$, was analyzed using a reduced major axis regression. To study the interaction between productivity ($PC1_P$), bottom water intensity (reconstructed by the $^{231}Pa/^{230}Th$ ratio; McManus et al., 2004; Böhm et al., 2015), and dissolution ($PC1_D$), a multiple linear regression was carried out.

RESULTS

Sediments from core SAT-048A represent hemipelagic muds rich in carbonate. The average grain size of the samples is slightly sandy mud, and in general, ranges from slightly clayey mud to muddy sand in some cases. The recovered sediments correspond to the latest Pleistocene and early/middle Holocene muds of the Imbé formation. The age model (**Supplementary Material**) indicates sample ages ranging from 43 to 5 ka.

Planktonic Foraminifera species indicate two contrasting temporal distribution patterns: 1) species with higher abundances during the Late Pleistocene that decreased in abundance towards the Holocene, *Globigerinita glutinata* (**Figure 2C**), *Globigerina bulloides*, *Globoconella inflata*, and *Neogloboquadrina incompta* (**Supplementary Material**); 2) species with lower abundance values during the Late Pleistocene and higher abundances in the Holocene, *Globigerinoides ruber albus* and *G. ruber ruber*, *Trilobatus sacculifer*, *Globorotalia menardii*, *Globigerinella calida*, *Orbulina universa*, *Globorotalia tumida*, and *Globigerinoides conglobatus* (**Supplementary Material**).

The performance of the MAT (shown in the **Supplementary Material**) was generally very good, with an R^2 of 0.993. The annual mean paleo-SST_{100m} estimates for core SAT-048A are shown in **Figure 2E** (residuals shown in **Supplementary Material**). The annual mean reconstructions show lower values from the bottom of the core until 37 ka (on average 16°C), although the lowest value occurred at 25 ka (15.2°C). For the 37–15 ka period, the observed temperature variation was larger and fluctuated faster than during the rest of the record, spanning from 15 to 19°C. A warming trend is indicated to have occurred before the Last Glacial Maximum (LGM) at 25 ka, with values between 19 and 23°C and the warmest SST_{100m} value (22.5°C) observed at 7 ka.

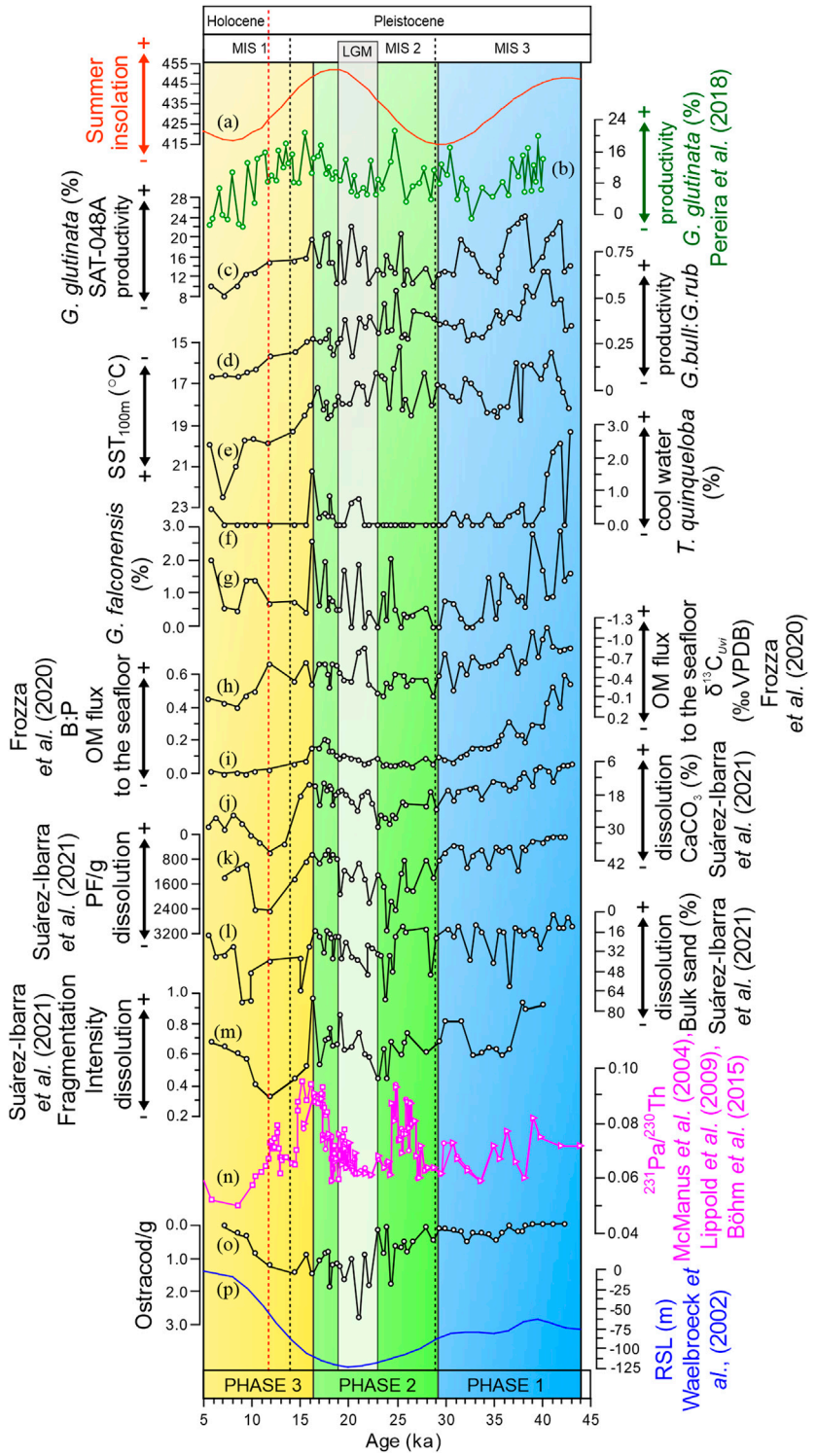

FIGURE 2 | Fluctuations in summer insolation, paleoenvironmental proxies for surface productivity, organic matter (OM) flux to the seafloor, $CaCO_3$ dissolution, Atlantic Meridional Overturning Circulation (AMOC) speed, and relative sea level. **(A)** Austral summer (February) insolation at 31° S (Laskar et al., 2004) **(B–C)** relative abundance of *G. glutinata* in cores GeoB2107-3 (b; Pereira et al., 2018) and SAT-048A (c; this study); **(D)** *G. bulloides*/*G. ruber* ratio (*G.bull*:*G.rub*); **(E)** SST_{100m} (°C) **(F–G)** relative abundance of *T. quinqueloba* (f) and *G. falconensis* (g); **(H)** $\delta^{13}C_{Uvi}$ (‰); **(I)** Benthic/Planktonic Foraminifera ratio (B:P) **(J)** $CaCO_3$ content of the sediment **(K)** number of planktonic Foraminifera tests per gram of sediment (PF/g) **(L)** sand bulk content (%) **(M)** fragmentation intensity **(N)** $^{231}Pa/^{230}Th$ values from McManus et al. (2004; squares), Lippold et al. (2009; circles), and Böhm et al. (2015; triangles) **(O)** Ostracods per gram of sediment (valves/g) **(P)** relative sea level (RSL; Waelbroeck et al., 2002). Note the inverted *y*-axes in (f), (g), and (i–k) to aid visualization. Proxies printed in black belong to sediment core SAT-048A. The three phases indicated in the plot are based on a principal component analysis of all productivity values, as shown in **Figure 3**.

All reconstructed paleoenvironmental proxies are shown in **Figure 2**. Paleo-productivity shows highest values in the 43–32/34 ka interval (superimposed on a decreasing trend), when reconstructed from *G. glutinata* abundances (**Figure 2C**) and the *G. bull*:*G.rub* ratios (**Figure 2D**), respectively. A relative plateau is witnessed for both proxies from 32/34 to 25 ka. The following time interval (25–17 ka) is characterized by an increasing trend. From 17 to 5 ka, *G. glutinata* and the *G. bull*:*G.rub* ratio show a decreasing trend with some of the lowest values of the entire record. The abundance of ostracods valves (**Figure 2**) is low during the 43–27 ka interval, then increases until 10 ka, and decreases afterward.

We ran a Spearman rank-order correlation to test the relationship between different productivity and dissolution proxies (**Table 1**). When the correlation was significant at the α = 0.05-level, the correlation coefficients ρ were categorized as either weak ($|\rho|$ = 0–0.33), medium ($|\rho|$ = 0.34–0.66), or strong ($|\rho|$ = 0.67–1). The paleo-productivity proxies *G. bull*/*G.rub* and *G. glutinata* (%) are not significantly correlated (p = 0.556), nevertheless, the correlations between productivity and OM flux proxies are all significant, ranging from medium to strong correlations. All the dissolution proxies are significantly correlated, also ranging from medium to strong. The correlation between productivity, OM flux and dissolution proxies are all significant, ranging from weak to strong relations, except for the FI vs *G. glutinata* (%) and the bulk sand (%) vs *G. glutinata* (%) proxies. The OM flux proxy Ostracod valves only showed a medium correlation with the *G. bull*/*G.rub* proxy and was also weakly–moderately correlated to three dissolution proxies.

These results indicate that all these proxies are also influenced by other environmental parameters, not just productivity and dissolution, respectively. Therefore, not any single proxy is suitable to provide an unbiased picture of the past environment. We, thus, aimed to develop synthetic productivity and dissolution proxies by combining all information in a PCA, which on its first axis amplifies the direction of largest variation in both parameters. PCAs were run both for productivity/OM flux (*G.bull*/*G.rub*, *G. glutinata* (%), $\delta^{13}C_{Uvi}$, and B:P; PCA_P) and dissolution proxies ($CaCO_3$, FI, PF/g, and bulk sand (%), PCA_D) on the data centered at zero and scaled to unit variance (**Supplementary Material**). The first principal component of the productivity/OM flux analysis ($PC1_P$) explains 62.14% of the variance in the data, while the first principal component for the dissolution proxies ($PC1_D$) captures 74.88% of data variance. The trends of $PC1_P$ and $PC1_D$ are shown in **Figure 3**, where the borders between three phases are based on the best solution of a set of piecewise OLS regressions with combinations of 70 feasible phase border scenarios. The loadings of the components on the principal component axes and the individual R^2-values from the piecewise regressions on which the phase borders are based are shown in the **Supplementary Material**. The optimal phase borders were determined by the R^2-product of 0.251 as follows: phase 1 (42.32–29.12 ka), where $PC1_p$ values decreased, indicating a reduction in productivity; phase 2 (28.56–16.15 ka), with stable to slightly increasing paleo-productivities; and phase 3 (15.51–5.77 ka), where productivity decreased again during the Holocene.

A reduced major axis regression between summer insolation and $PC1_P$ (**Supplementary Material**) yielded a significant (p < 0.001) correlation value of 0.476. A multiple linear regression between the independent variable $PC1_P$ and bottom water velocity ($^{231}Pa/^{230}Th$) and $PC1_D$ as dependent variable was carried out and results are shown in **Table 2**. Only $PC1_P$ is

TABLE 1 | Correlation coefficient (ρ) and statistical significance (p) for productivity and dissolution indices in sediment core SAT-048A from the western South Atlantic. *G. glutinata* (%): Relative abundance of *Globigerinita glutinata*; $\delta^{13}C_{Uvi}$: VPDB $\delta^{13}C$-values of shells of the benthic foraminifer genus *Uvigerina*; B:P: Ratio between benthic and planktonic Foraminifera; $CaCO_3$ (%): Relative $CaCO_3$ content of the sediment; FI: Planktonic foraminifera fragmentation intensity; PF/g: Number of Planktonic foraminiferal tests per gram of sediment; bulk sand (%): Relative sand content of the sediment; Ostracod valves: Number of Ostracod valves per Gram of sediment. Significant p-values (at α = 0.05) are highlighted in bold; for these, the correlation coefficient was marked as weak (italics), medium (bold), or strong (bold-italics).

	—	*G.bull/ G.rub*	*G. glutinata* (%)	$\delta^{13}C_{Uvi}$	B:P	$CaCO_3$ (%)	FI	PF/g	Sand bulk (%)
G. glutinata (%)	ρ	0.086	—	—	—	—	—	—	—
	p	0.556	—	—	—	—	—	—	—
$\delta^{13}C_{Uvi}$	ρ	**–0.441**	**–0.508**	—	—	—	—	—	—
	p	**0.002**	**<0.001**	—	—	—	—	—	—
B:P	ρ	**0.458**	**0.511**	***–0.795***	—	—	—	—	—
	p	**0.001**	**<0.001**	**<0.001**	—	—	—	—	—
$CaCO_3$ (%)	ρ	**–0.518**	**–0.430**	0.777	***–0.914***	—	—	—	—
	p	**<0.001**	**0.002**	**<0.001**	**<0.001**	—	—	—	—
FI	ρ	*0.329*	0.287	*–0.304*	**0.452**	**–0.567**	—	—	—
	p	**0.024**	**0.05**	**0.038**	**0.001**	**<0.001**	—	—	—
PF/g	ρ	**–0.371**	*–0.302*	***0.703***	***–0.811***	***0.831***	**–0.53**	—	—
	p	**0.009**	**0.035**	**<0.001**	**<0.001**	**<0.001**	**<0.001**	—	—
Sand bulk (%)	ρ	**–0.389**	–0.204	**0.473**	**–0.579**	**0.629**	**–0.606**	**0.576**	—
	p	**0.006**	0.16	**0.001**	**<0.001**	**<0.001**	**<0.001**	**<0.001**	—
Ostracod valves	ρ	**–0.354**	0.129	0.187	–0.229	0.24	**–0.334**	**0.479**	**0.304**
	p	**0.015**	0.387	0.207	0.121	0.104	**0.022**	**0.001**	**0.038**

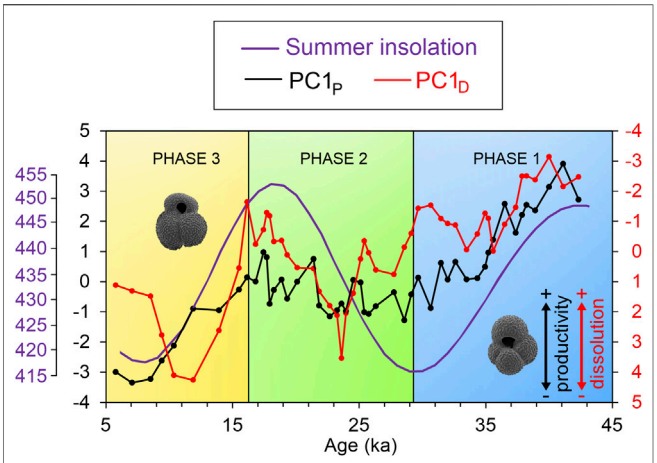

FIGURE 3 | Mean average for the first principal components of principal component analyses on all productivity proxies ($PC1_P$, black line) and all dissolution proxies ($PC1_D$, red line) in samples from sediment core SAT-048A in the South Atlantic. The purple line represents the Austral summer (February) insolation at 31° S (Laskar et al., 2004). The three phases defined by productivity trends (decreasing in phases 1 and 3, increasing in phase 2) are indicated. Dominant species of planktonic Foraminifera (*Globigerina bulloides* in phase 1, *Globigerinoides ruber* in phase 3) are indicated.

significantly influencing dissolution, and explains around 51% of the observed dissolution signal.

DISCUSSION

Radiocarbon Reversals

The occurrence of reversals in planktonic Foraminifera radiocarbon dates are not rare in the studies of the south Brazilian continental margin (SBCM, e.g., Sortor and Lund, 2011; Hoffman and Lund, 2012; Portilho-Ramos et al., 2019), being related either to: 1) morphological features of the sea bottom that remobilize sediments (such as turbidity or contour currents), or to 2) post-depositional chemical processes that affect the ^{14}C concentrations. The age model of core SAT-048A here presented (**Supplementary Figure S3**) indicates three intervals where samples yielded mean older ages (**Supplementary Table S3**). Nevertheless, the only significant difference is shown in the sample at 183.5 cm depth (31.1 ka before calibration), between 217 and 149 cm (27.8–22.7 ka), an interval constituted by hemipelagic mud rich in carbonate. According to Kowsmann et al. (2014), features of geological instability for the SBCM usually occurred between 28 and 15 ka, during relative low sea levels. Nevertheless, reversals of AMS ^{14}C planktonic Foraminifera dates from core SAT-048A are not associated to abrupt changes on the grain size record (**Supplementary Figure S4**). Moreover, the action of contour currents in the proximities of the study area (Viana, 2001; Duarte and Viana, 2007; Hernández-Molina et al., 2016) could, have gradually remobilized older particles (such as planktonic Foraminifera shells), masking the ^{14}C ages and increasing the temporal mixing.

Regarding the chemical processes, Rodrigues et al. (2020) reported older radiocarbon dates likely due to the upward migration of ^{14}C-depleted methane fluids from gas chimneys, as already reported for the south portion of the SBCM (Portilho-Ramos et al., 2018; Ketzer et al., 2020), which can precipitate in shell interstitial pores (Wycech et al., 2016), producing an alteration in the radiocarbon dates. Given the above, we tried to diminish the impact of radiocarbon reversals by using 1) a high number of correlation points (10 radiocarbon dates and one geomagnetic correlation point) and, 2) the *rbacon* package for software R, which implements Bayesian statistics that calculate mean ages for age model constructions, and has the capacity to deal with ^{14}C reversals.

Sea Surface Productivity

Three phases were defined from the $PC1_P$ trends (**Figure 3**). Phases 3 and 1 fall into time intervals with decreasing summer insolation values, while phase 2 is characterized by increasing summer insolation. The correlation between $PC1_P$ and summer insolation values is supported by the significant ($p < 0.001$) values of a reduced major axis regression ($r = 0.476$). This is supported by mechanisms, reported in the literature, that drove the paleo-productivity changes in the western South Atlantic. Portilho-Ramos et al. (2019) explained the high glacial productivity by a combination of short – but highly productive – austral summer upwelling periods and prolonged winter conditions favorable to the intrusion of RdlPE.

The short summer upwelling periods resulted from the enhanced northeasterly (NE) winds blowing along the shore during intervals with high summer insolation, both directly, by pushing surface waters offshore due to the Ekman transport (Chen et al., 2019), and indirectly by strengthening the BC meandering and, therefore, enhancing shelf break upwelling (Portilho-Ramos et al., 2015; Pereira et al., 2018). This interpretation is supported by the observed changes in the relative abundances of: 1) *Globigerinita glutinata* (Conan and Brummer, 2000; Souto et al., 2011), a species that feeds on

TABLE 2 | Results from a multiple linear regression between summarized paleo-productivity ($PC1_P$; first axis of a principal component analysis including all correlatable productivity proxies) and bottom water velocity $^{231}Pa/^{230}Th$ and summarized dissolution (first axis of a principal component analysis including all dissolution proxies) as dependent variable for sediment core SAT-048A from the South Atlantic. *p*-values significant at $\alpha = 0.05$ are indicated in bold.

	Coefficient	Standard error	*t*	*p*	R^2	*r*
Constant	0.286	1.425	0.201	0.842	—	—
$PC1_P$	−0.781	0.122	−6.402	**<0.001**	0.519	0.720
$^{231}Pa/^{230}Th$	−4.141	20.458	−0.202	0.840	0.091	0.302

diatoms (Schiebel and Hemleben, 2017) and therefore benefits from the glacial silicic acid-rich SACW intrusions in the area (Portilho-Ramos et al., 2019) (**Figure 2B,C**); 2) *Turborotalita quinqueloba*, which is associated with stronger intrusions of cooler SACW into the photic zone (Souto, et al., 2011; Lessa et al., 2014, 2016) (**Figure 2F**); and 3) *Globigerina falconensis*, which is associated with eutrophic conditions (Sousa et al., 2014) (**Figure 2G**). Additionally, a reconstructed SST_{100m} cooler than 20°C (Campos et al., 2000; Silveira et al., 2000; Castelão et al., 2004) along with a *G. bull*:*G.rub* ratio higher than 0.25 (Lessa et al., 2014) for the Pleistocene portion of the record indicates a constant presence of the SACW in the subsurface during the short austral upwelling of the late glacial.

Prolonged winter conditions involved prevalent southwesterly (SW) winds year-round which carried outflows from the Río de La Plata (RdlPE) (Pimenta et al., 2005; Piola et al., 2005) and other continental sources (Camaquã, Jaguarão, and Jacuí rivers)—presently converging in the PMLS–closer to the study area (Piola et al., 2000; Nagai et al., 2014). Strengthened SW winds would also displace the BMC to a location closer to the area (Gonzalez-Silvera et al., 2006), which is supported by the higher relative abundances of *Globoconella inflata* and *Neogloboquadrina incompta* (**Supplementary Material**). The abundances of these two species can be interpreted as an indicator for a BMC closer to the study area (Boltovskoy et al., 1996), induced by the enhanced SW winds during the late last glacial.

Several authors suggest that during low relative sea levels (glacial times), periods of higher nutrient availability and increased terrigenous sediment input were favored due to the more offshore position of the BC and the exposure of the continental shelf (Mahiques et al., 2007; Gu et al., 2017; Pereira et al., 2018, Portilho-Ramos et al., 2019). Moreover, the Río de la Plata (Lantzsch et al., 2014) and Jacuí and Camaquã river paleo-drainages (Weschenfelder et al., 2014) were closer to the study area during this interval (higher influence of the PMLS). Higher Fe/Ca values (Heil, 2006), higher relative abundances of eutrophile dinoflagellate cysts species (Gu et al., 2017), and high terrestrial palynomorph proportions (Bottezini et al., 2022), are all evidence of the greater influence of continental outflow in the study area under lower relative sea levels during the late last glacial (which approximately corresponds to our phases 1 and 2). Medium paleo-productivity estimates during the LGM (relative sea level approximately 120 m lower; **Figure 3**) stand in contrast to the higher sea levels during phase 1 (relative sea level approximately 75 m below, Waelbroeck et al., 2002), where higher (terrigenous-related) fertilization was expected due the lower eustatic sea level. This suggests a different influence for the continental terrigenous fertilization for mid-depth cores retrieved from the continental slope. In contrast, for the Holocene, the higher relative sea level and onshore displacement of the BC, as well as the absence of the SACW, inhibited the photic zone fertilization, leading to oligotrophic conditions (Mahiques et al., 2007), witnessed in the phase 3.

Organic Matter Flux to the Seafloor and Carbonate Dissolution

Orbital to suborbital climate cycles can influence the abundance of deep-sea benthic communities (Cronin et al., 1999). Since abundance fluctuations of benthic Foraminifera and ostracods are related to variations in particulate organic carbon fluxes to the seafloor (Smith et al., 1997; Rex et al., 2006; Rex and Etter, 2010), their use as surface paleo-productivity indicators is widespread (Nees et al., 1999; Herguera, 2000; Rasmussen et al., 2002; Gooday, 2003; Yasuhara et al., 2012). The surface productivity fluctuations, indicated by the *G. glutinata* abundance and *G. bull*:*G.rub*, are significantly correlated to those of the OM flux recorded by the B:P ratio and the $\delta^{13}C_{Uvi}$ (**Table 1**). This effective OM export from the surface to the seafloor revealed a high benthic–pelagic coupling (Toledo et al., 2007). The B:P changes are accompanied by a similar trend in inverse $\delta^{13}C_{Uvi}$ (**Figure 2H,I**), which are expected to decrease when higher OM fluxes, rich in ^{12}C due to the preferential incorporation of the light isotope during photosynthesis (Wefer et al., 1999), reach the seabed (Ravello and Hillaire-Marcel, 2007). Nevertheless, the abundance of ostracod valves (**Figure 2**) was only significantly correlated with *G. bull*:*G. rub* ratio values. Intriguingly, ostracod valves showed a hump-shaped relation with productivity (Yasuhara et al., 2012), where values increased under moderate OM supply and declined under very low and very high productive conditions. This is because under high-productivity scenarios, oxygen levels at the sea floor tend to decrease and deep-sea ostracods, which are mostly epifaunal (Jöst et al., 2017), would not respond well to such an environment. On the other hand, ostracods valves had a significant ($p > 0.001$) strong correlation ($\rho = -0.701$) with paleo-bathymetric variations, where abundances decreased exponentially with water depth increase (Rex et al., 2006; Rex and Etter, 2010).

Dissolution indicators suggest higher calcium carbonate dissolution during the beginning of Phases 1 and the transition of phases 2 and 3 (**Figure 2**, **3**), related to the OM flux. Enhanced dissolution could theoretically be triggered by two different processes: 1) increase in CO_2 concentrations (decreasing the water pH) due to the remineralization of OM at the seafloor (Jahnke et al., 1997; Schiebel, 2002) or 2) changes in the bottom water mass configuration related to AMOC dynamics (speed or geometry). Although the B:P ratios are also used as a dissolution indicator (Berger and Diester-Haass, 1988; Conan et al., 2002), Kučera (2007) states that this is only applicable for abyssal depths. We also have evidence from regional studies (Petró et al., 2018b) that benthic foraminifera are more prone to dissolution in this setting than planktonic foraminifers. This means that our observed B:P ratios are, in the worst case, an underestimate of the real situation because dissolution would attenuate it.

In the SBCM basins, the $\delta^{13}C_{Uvi}$ values have been used to infer oscillations of OM input (Toledo et al., 2007; Dias et al., 2018; Rodrigues et al., 2018; Frozza et al., 2020). Nevertheless, $\delta^{13}C_{Uvi}$ values are influenced by several factors, such as

accumulation rates of organic carbon, regional changes of water masses, the global carbon cycle, photosynthesis respiration processes, temperature, and pH (Ravelo and Hillaire-Marcel, 2007; Hesse et al., 2014). Calcite dissolution has, in contrast, no influence on the foraminiferal $\delta^{13}C$ (Petró et al., 2018b). Lund et al. (2015) suggested that lower values of benthic $\delta^{13}C$ during glacial times are associated with a weak AMOC. Nevertheless, the fluctuations of $\delta^{13}C_{Uvi}$ and the carbonate preservation could be the result of the interplay between the OM flux and water masses changes.

Based on εNd in planktonic Foraminifera at mid-depths in the western South Atlantic, Howe et al. (2016, 2018) showed variations of water masses at intermediate depths of 1,000–1,200 m (cores GeoB2107-3 and KNR159-3-36GGC) during the Holocene, and at 2,200 m (core GL-1090) since Heinrich Stadial 1. After the Heinrich Stadial 1, core GL-1090s εNd values decreased, becoming less radiogenic and more related to modern upper NADW values, while cores GeoB2107-3's and KNR159-3-36GGC's εNd values increased after about 10 ka, becoming more radiogenic and showing more affinity with modern AAIW. Sediment core GeoB2104-3 (1,500 m) is located between these aforementioned cores, at the same depth as sediment core SAT-048A on which the present study is based, at its εNd values remained stable during the 25–4 ka interval (Howe J. N. W. et al., 2016). This indicates that SAT048A's $\delta^{13}C_{Uvi}$ fluctuations were produced by the OM bottom flux rather than water masses reconfigurations–at least throughout the studied time interval.

In addition, the $^{231}Pa/^{230}Th$ ratio (**Figure 2N**) has been used to track the intensity of the AMOC (McManus et al., 2004; Lippold et al., 2009; Böhm et al., 2015), where lower values indicate a strengthened AMOC. During periods of high $^{231}Pa/^{230}Th$ values and indicating AMOC slowdown (like Heinrich Stadials), a higher concentration of respired CO_2 is accumulated in seafloor water masses. As proposed by Howe JN. et al. (2016), this is a possible explanation for the intervals of increased calcium carbonate dissolution. Nevertheless, the results from the multiple linear regression (**Table 2**) point to paleo-productivity as the main factor to influence dissolution. The multiple linear regression designates the sea surface productivity and OM flux to the seafloor as the principal agents of the calcium carbonate dissolution (**Figure 4**), at least for the 25–4 ka interval, which is related to changes in the summer insolation. This is true, even including the decoupling between productivity and dissolution visible in our data during the last ca. 5 kyrs (**Figure 3**). We hypothesize that the increasing dissolution at constantly low productivity, high AMOC rates (**Figure 2N**) and stable water mass configuration during this last segment of the record is related to the rising temperatures in this period, which increased the Mg/Ca values of the biogenic carbonate. Since higher Mg content facilitates dissolution of calcite, shells produced during this time would be more prone to dissolution, so that other environmental parameters were no longer the major factors that affected calcite dissolution. Future studies should investigate possible changes in bottom water mass configuration through εNd isotopes for the entire

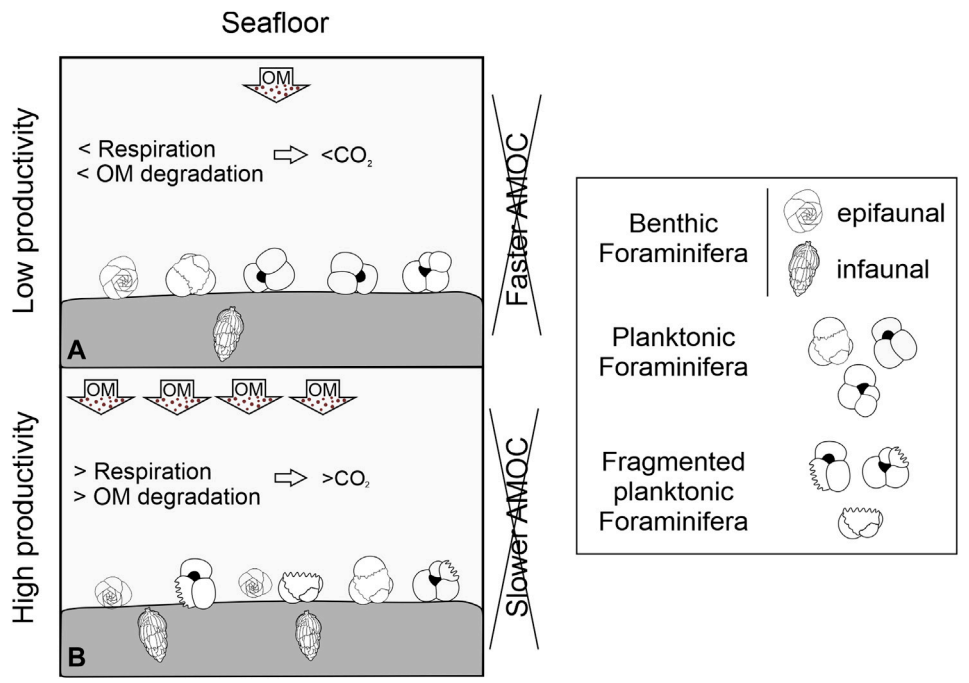

FIGURE 4 | Schematic representation of two possible end-member scenarios affecting carbonate dissolution on deep-water assemblages of sediment core SAT-048A (South Atlantic). The paleoceanographic changes could be triggered by: **(A)** Low organic matter (OM) inputs to the seafloor, which results in lower benthic abundances and better preservation of $CaCO_3$, or **(B)** high OM input that increases benthic abundances and CO_2 concentrations, decreases the seawater pH, and dissolves the planktonic Foraminifera tests (fragmentation on benthic Foraminifera was not assessed).

studied section to 1) increase our understanding of productivity-related carbon dissolution at the sea floor and 2) quantify the impact of changes of the biological pump on the total organic carbon and biogenic carbonates burial. This will considerably aid the understanding of the glacial inorganic carbon sequestration.

CONCLUSION

Planktonic Foraminifera assemblages from sediment core SAT-048A, along with geochemical analyses and sedimentological data, enabled us to reconstruct the surface and bottom water conditions that occurred during the last 43 kyrs in the western South Atlantic, and to contextualize the related production-dissolution processes in the area. The Pleistocene–Holocene transition was characterized by a shift from a glacial eutrophic environment to more oligotrophic post-glacial conditions, as suggested by the *G. bull*:*G.rub* ratio and the SST_{100m}, where intrusions of the nutrient-rich SACW were inhibited and the RdlPE and local river discharges (nowadays PMLS) were placed further away from the core site. The orbital-scale fluctuations of the upwelling dynamics (indicated by the relative abundances of *G. glutinata* and *T. quinqueloba*), modulated by insolation and NE wind changes, directly influenced the surface productivity and the OM fluxes to the seafloor (as shown by the B:P ratio and $\delta^{13}C_{Uvi}$). Imposed on the mechanisms behind the glacial–interglacial changes, stronger NE winds, generated by higher summer insolation, fertilized the photic zone, strengthened the BC, increased meandering, and enhanced intrusion of cooler and nutrient-richer waters into the subsurface layers. The enhanced upwelling conditions were also registered at the sea floor, where the bacterial decomposition of OM and the respiration of higher abundances of benthic communities increased the CO_2 concentration, which created more acidic conditions that caused different levels of carbonate dissolution, evidenced in the fragmentation of the planktonic Foraminifera tests. While changes in the bottom water masses could hypothetically cause the calcium carbonate dissolution, εNd analyses in a nearby sediment core at the same depth suggest no changes in the bottom water mass influence for the 25–4 ka interval, pointing to sea surface productivity and the intensity of the AMOC as possible causes of the carbonate dissolution. A multiple linear regression between summarized productivity and $^{231}Pa/^{230}Th$ (proxy for AMOC intensity), indicates that productivity is the main controlling factor of calcium carbonate dissolution. The continental influence (i.e., terrigenous input) must be better assessed in future studies, since, in contrast to expectations, no increased productivity was registered during the lowest relative sea level (LGM), when terrestrial input should have been highest. The dissolution of planktonic Foraminifera tests, induced by an enhanced biological pump (evidenced in the high glacial surface productivity and the high OM fluxes to the sea floor), must call the attention to future research, since a strong biological pump influences biogenic carbonate burial and CO_2 sequestration and burial at the seafloor.

DATA AVAILABILITY STATEMENT

The original contributions presented in the study are included in the article/**Supplementary Material**, further inquiries can be directed to the corresponding author.

AUTHOR CONTRIBUTIONS

JYSI and MAGP conceptualized the study; JYSI curated the data; JYSI conducted the formal analyses; MAGP and MFGW acquired funding; JYSI, CFF and PLP investigated the samples; JYSI, CFF, MFGW, MAGP developed the methods; MAGP provided the resources; MFGW and MAGP supervised the project; MFGW and MAGP validated the results; JYSI visualized the results; JYSI wrote the original draft; JYSI, CFF, PLP, SMP, MFGW, and MAGP reviewed and edited the manuscript.

FUNDING

This work was supported by the Brazilian Coordination of Higher Education Staff Improvement (CAPES) (grant number 88887.091729/2014-01), the Brazilian National Council for Scientific and Technological Development (CNPq) (grant number 407922/2016-4) and the PRIMUS program (grant number PRIMUS/20/SCI/019) and PROGRES Q45 grants, Charles University. JS-I was supported by the CNPq (MSc) and the STARS programs (PhD) from the Charles University, respectively. CF was supported by the CAPES (PhD).

ACKNOWLEDGMENTS

The authors are grateful to Gilberto Griep (*in memoriam*) for his commitment to making sediment cores retrieved for the industry available to the scientific community. We thank Dr. Igor Venâncio (Instituto Nacional de Pesquisas Espaciais, Brazil), Dr. João Coimbra (Universidade Federal do Rio Grande do Sul, Brazil), Dr. Geise dos Anjos Zerfass (Petróleo Brasileiro S.A., Brazil), Editor Dr. Jacek Raddatz and two reviewers, Dr. Selvaraj and Dr. Patrick Grunert for comments and suggestions that helped to improve this manuscript.

SUPPLEMENTARY MATERIAL

The Supplementary Material for this article can be found online at: https://www.frontiersin.org/articles/10.3389/feart.2022.830984/full#supplementary-material

REFERENCES

Bé, A. W. H. (1967). Foraminifera Families: Globigerinidae and Globorotaliidae, Conseil Permanent International Pour L'exploration De La Mer, Zooplankton. *Charlottenlund, Denmark: Conseil Int. pour l'Exploration*

Bé, A. W. H., Hemleben, C., Anderson, O. R., Spindler, M., Hacunda, J., Tuntivate-Choy, S., et al. (1977). Laboratory and Field Observations of Living Planktonic Foraminifera. *Micropaleontology* 23 (2), 155–179. doi:10.2307/1485330

Berger, W. H., Bonneau, M. C., and Parker, F. L. (1982). Foraminifera on the Deep-Sea Floor: Lysocline and Dissolution Rate. *Oceanologica acta* 5 (2), 249.

Berger, W. H., and Diester-Haass, L. (1988). Paleoproductivity: the Benthic/planktonic Ratio in Foraminifera as a Productivity index. *Mar. Geology.* 81, 15–25. doi:10.1016/00254813227(88)90014-X

Berger, W. H. (1970). Planktonic Foraminifera: Selective Solution and the Lysocline. *Mar. Geology.* 8, 111–138. doi:10.1016/0025-3227(70)90001-0

Blaauw, M., and Christen, J. A. (2011). Flexible Paleoclimate Age-Depth Models Using an Autoregressive Gamma Process. *Bayesian Anal.* 6 (3), 457–474. doi:10.1214/1148410.1214/ba/1339616472

Böhm, E., Lippold, J., Gutjahr, M., Frank, M., Blaser, P., Antz, B., et al. (2015). Strong and Deep Atlantic Meridional Overturning Circulation during the Last Glacial Cycle. *Nature* 517, 73–76. doi:10.1038/nature14059

Bolli, H. M., and Saunders, J. B. (1989). "Oligocene to Holocene Low Latitude Planktic Foraminifera," in *Plankton Stratigraphy* (K. Cambridge Earth Sciences SeriesCambridge University Press), 1, 155

Boltovskoy, E., Boltovskoy, D., Correa, N., and Brandini, F. (1996). Planktic Foraminifera from the Southwestern Atlantic (30 °-60 °S): Species-specific Patterns in the Upper 50 M. *Mar. Micropaleontology* 28, 53–72. doi:10.1016/0377-8398(95)00076-3

Bottezini, S. R., Leonhardt, A., Diniz, D., and Gonçalves, J. F. (2022). Climatic and Vegetational Dynamics in Southern Brazil between 47.8 and 7.4 Cal Ka BP: a Palynological Analysis. *Revista Brasileira de Paleontologia* 24 (4), 345–356. doi:10.4072/rbp.2021.4.05

Brummer, G. J. A., and van Eijden, A. J. M. (1992). "Blue-ocean" Paleoproductivity Estimates from Pelagic Carbonate Mass Accumulation Rates. *Mar. Micropaleontology* 19, 99–117. doi:10.1016/0377-8398(92)90023-D

Campos, E. J. D., Gonçalves, J. E., and Ikeda, Y. (1995). Water Mass Characteristics and Geostrophic Circulation in the South Brazil Bight: Summer of 1991. *J. Geophys. Res.* 100 (9), 18537–18550. doi:10.1029/95jc01724

Campos, E. J. D., Velhote, D., and da Silveira, I. C. A. (2000). Shelf Break Upwelling Driven by Brazil Current Cyclonic Meanders. *Geophys. Res. Lett.* 27, 751–754. doi:10.1029/1999GL010502

Castelão, R. M., Campos, E. J. D., and Miller, J. L. (2004). A Modelling Study of Coastal Upwelling Driven by Wind and Meanders of the Brazil Current. *J. Coastal Res.* 203, 662–671. doi:10.2112/1551-5036(2004)20662AMSOCU2.0.CO;2

Chen, H.-H., Qi, Y., Wang, Y., and Chai, F. (2019). Seasonal Variability of SST Fronts and Winds on the southeastern continental Shelf of Brazil. *Ocean Dyn.* 69, 1387–1399. doi:10.1007/s10236-019-01310-1

Conan, S. M.-H., and Brummer, G. J. A. (2000). Fluxes of Planktic Foraminifera in Response to Monsoonal Upwelling on the Somalia Basin Margin. *Deep Sea Res. Part Topical Stud. Oceanography* 47 (9-11), 2207–2227. doi:10.1016/s09670645(00)00022-99

Conan, S. M.-H., Ivanova, E., and Brummer, G. J. (2002). Quantifying Carbonate Dissolution and Calibration of Foraminiferal Dissolution Indices in the Somali Basin. *Mar. Geology.* 182 (3-4), 325–349. doi:10.1016/s0025-3227(01)00238-9

Cronin, T. M., De Martino, D. M., Dwyer, G. S., and Rodriguez-Lazaro, J. (1999). Deepsea Ostracode Species Diversity: Response to Late Quaternary Climate Change. *Mar. Micropaleontology* 37 (3-4), 231–249. doi:10.1016/S0377-8398(99)00026-2

de Almeida, F. K., de Mello, R. M., Rodrigues, A. R., and Bastos, A. C. (2022). Bathymetric and Regional Benthic Foraminiferal Distribution on the Espírito Santo Basin Slope, Brazil (SW Atlantic). *Deep Sea Res. Oceanographic Res. Pap.* 181, 103688. doi:10.1016/j.dsr.2022.103688

de Oliveira Lessa, D. V., Ramos, R. P., Barbosa, C. F., Da Silva, A. R., Belem, A., Turcq, B., et al. (2014). Planktonic Foraminifera in the Sediment of a Western Boundary Upwelling System off Cabo Frio, Brazil. *Mar. Micropaleontology* 106, 55–68. doi:10.1016/j.marmicro.2013.12.003

Dias, B. B., Barbosa, C. F., Faria, G. R., Seoane, J. C. S., and Albuquerque, A. L. S. (2018). The Effects of Multidecadal-Scale Phytodetritus Disturbances on the Benthic Foraminiferal Community of a Western Boundary Upwelling System, Brazil. *Mar. Micropaleontology* 139, 102–112. doi:10.1016/j.marmicro.2017.12.003

Duarte, C. S. L., and Viana, A. R. (2007). Santos Drift System: Stratigraphic Organization and Implications for Late Cenozoic Palaeocirculation in the Santos Basin, SW Atlantic Ocean. *Geol. Soc.* 276, 171–198. doi:10.1144/GSL.SP.2007.276.01.09

EPICA Community Members. (2004). Eight Glacial Cycles from an Antarctic Icecore. *Nature* 429, 623–628. doi:10.1038/nature02599

Frenz, M., Höppner, R., Stuut, J.-B. W., Wagner, T., and Henrich, R. (2003). Surface Sediment Bulk Geochemistry and Grain-Size Composition Related to the Oceanic Circulation along the South American Continental Margin in the Southwest Atlantic. In: *The South Atlantic in the Late Quaternary*, *Wefer, G., Mulitza, S., Ratmeyer. V.*, Springer-Verlag, Berlin, Heidelberg, New York, Tokyo, v. (eds), pp. 347–373.doi:10.1007/978-3-642-18917-3_17

Frenz, M., and Henrich, R. (2007). Carbonate Dissolution Revealed by silt Grain-Size Distribution: Comparison of Holocene and Last Glacial Maximum Sediments from the Pelagic South Atlantic. *Sedimentology* 54, 391–404. doi:10.1111/j.1365-3091.2006.00841.x

Frozza, C. F., Pivel, M. A. G., Suaáez-Ibarra, J. Y., Ritter, M. N., and Coimbra, J. C. (2020). Bioerosion on Late Quaternary Planktonic Foraminifera Related to Paleoproductivity in the Western South Atlantic. *Paleoceanography and Paleoclimatology*, e2020PA003865. doi:10.1029/2020pa003865

Gonzales, M. V., de Almeida, F. K., Costa, K. B., Santarosa, A. C. A., Camillo, E., de Quadros, J. P., et al. (2017). Help Index: Hoeglundina Elegans Preservation Index for Marine Sediments in the Western South Atlantic. *J. Foraminiferal Res.* 47, 56–69. doi:10.2113/gsjfr.47.1.56

Gonzalez-Silvera, A., Santamaría-del-Angel, E., and Millán-Núñez, R. (2006). Spatial and Temporal Variability of the Brazil-Malvinas Confluence and the La Plata Plume as Seen by SeaWIFS and AVHRR Imagery. *J. Geophys. Res.* 111, C06010. doi:10.1029/2004JC002745

Gooday, A. J. (2003). Benthic Foraminifera (Protista) as Tools in Deep-Water Palaeoceanography: Environmental Influences on Faunal Characteristics. *Adv. Mar. Biol.* 46, 1–90. doi:10.1016/S0065-28810(03)46002-110.1016/s0065-2881(03)46002-1

Gooday, A. J. (2002). Biological Responses to Seasonally Varying Fluxes of Organic Matter to the Ocean Floor: A Review. *J. oceanography* 58, 305–332. doi:10.1023/A:1015865826379

Gordon, A. L., and Greengrove, C. L. (1986). Geostrophic Circulation of the Brazil-Falkland confluence. *Deep Sea Res. A. Oceanographic Res. Pap.* 33 (5), 573–585. doi:10.1016/0198-0149(86)90054-3

Gu, F., Zonneveld, K. A. F., Chiessi, C. M., Arz, H. W., Pätzold, J., and Behling, H. (2017). Long-term Vegetation, Climate and Ocean Dynamics Inferred from a 73,500 Years Old marine Sediment Core (GeoB2107-3) off Southern Brazil. *Quat. Sci. Rev.* 172, 55–71. doi:10.1016/j.quascirev.2017.06.028

Hales, B. (2003). Respiration, Dissolution and the Lysocline. *Paleoceanography* 18 (4), 1–14. doi:10.1029/2003PA000915

Hammer, O., David, A. T., and Paul, D. (2001). Past: Paleontological Statistics Software Package for Education and Data Analysis. *Palaeontol. Electronica* 4 (1), 1–9

Heil, G. M. N. (2006). Abrupt Climate Shifts in the Western Tropical to Subtropical Atlantic Region during the Last Glacial. PhD Thesis. *Universtity of Bremen* 121.

Hemleben, C., Spindler, M., and Anderson, O. R. (1989). New York: Estados Unidos de América: Springer. doi:10.1007/978-1-4612-3544-6Modern Planktonic Foraminifera

Herguera, J. C. (2000). Last Glacial Paleoproductivity Patterns in the Eastern Equatorial Pacific: Benthic Foraminifera Records. *Mar. Micropaleontology* 40 (3), 259–275. doi:10.1016/S0377-8398(00)00041-4

Hernández-Molina, F. J., Soto, M., Piola, A. R., Tomasini, J., Preu, B., Thompson, P., et al. (2016). A Contourite Depositional System along the Uruguayan continental Margin: Sedimentary, Oceanographic and Paleoceanographic Implications. *Mar. Geology.* 378, 333–349. doi:10.1016/j.margeo.2015.10.008

Hesse, T., Wolf-Gladrow, D., Lohmann, G., Bijma, J., Mackensen, A., and Zeebe, R. E. (2014). Modelling $\delta^{13}C$ in Benthic Foraminifera: Insights from Model Sensitivity Experiments. *Mar. Micropaleontology* 112, 50–61. doi:10.1016/j.marmicro.2014.08.001

Hoffman, J. L., and Lund, D. C. (2012). Refining the Stable Isotope Budget for Antarctic Bottom Water: New Foraminiferal Data from the Abyssal Southwest Atlantic. *Paleoceanography* 27, PA1213. doi:10.1029/2011PA002216

Hogg, N. G., Owens, W. B., Siedler, G., and Zenk, W. (1996). Circulation in the Deep Brazil BasinThe South Atlantic: Present and Past Circulation. in *Berlin Heidelberg*. Editors G. Wefer, W. H. Berger, G. Siedler, and D. J. Webb (Springer-Verlag), 13–44.

Howe, J. N., Piotrowski, A. M., Noble, T. L., Mulitza, S., Chiessi, C. M., and Bayon, G. (2016a). North Atlantic Deep Water Production during the Last Glacial Maximum. *Nat. Commun.* 7, 11765. doi:10.1038/ncomms11765

Howe, J. N. W., Huang, K.-F., Oppo, D. W., Chiessi, C. M., Mulitza, S., Blusztajn, J., et al. (2018). Similar Mid-depth Atlantic Water Mass Provenance during the Last Glacial Maximum and Heinrich Stadial 1. *Earth Planet. Sci. Lett.* 490, 51–61. doi:10.1016/j.epsl.2018.03.006

Howe, J. N. W., Piotrowski, A. M., Oppo, D. W., Huang, K. F., Mulitza, S., Chiessi, C. M., et al. (2016b). Antarctic Intermediate Water Circulation in the South Atlantic over the Past 25,000 Years. *Paleoceanography* 31, 1302–1314. doi:10.1002/2016PA002975

Hutson, W. H. (1980). The Agulhas Current during the Late Pleistocene: Analysis of Modern Faunal Analogs. *Science* 207, 64–66. doi:10.1126/science.207.4426.64

Jahnke, R. A., Craven, D. B., McCorkle, D. C., and Reimers, C. E. (1997). $CaCO_3$ Dissolution in California continental Margin Sediments: The Influence of Organic Matter Remineralization. *Geochimica et Cosmochimica Acta* 61 (17), 3587–3604. doi:10.1016/S00167037(97)00184-110.1016/s0016-7037(97)00184-1

Jöst, A. B., Yasuhara, M., Okahashi, H., Ostmann, A., Arbizu, P. M., and Brix, S. (2017). Vertical Distribution of Living Ostracods in Deep-Sea Sediments, North Atlantic Ocean. *Deep Sea Res. Part Oceanographic Res. Pap.* 122, 113–121. doi:10.1016/j.dsr.2017.01.012

Jouzel, J., Masson-Delmotte, V., Cattani, O., Dreyfus, G., Falourd, S., Hoffmann, G., et al. (2007). Orbital and Millennial Antarctic Climate Variability over the Past 800,000 Years. *Science* 317, 793–796. doi:10.1126/science.1141038

Kemle-von Mücke, S., and Hemleben, C. (1999). *Foraminifera*. Editors D. Boltovskoy (Leiden: Backhuys Publishers), 43–73

Ketzer, M., Praeg, D., Rodrigues, L. F., Augustin, A., Pivel, M. A. G., Rahmati-Abkenar, M., et al. (2020). Gas Hydrate Dissociation Linked to Contemporary Ocean Warming in the Southern Hemisphere. *Nat. Commun.* 11, 3788. doi:10.1038/s41467-020-17289-z

Kowsmann, R. O., Lima, A. C., and Vicalvi, M. A. (2014). Feições indicadoras de instabilidade geológica no talude continental e no Platô de São Paulo. in *Geologia e Geomorfologia*. Editor R. O. Kowsmann (Rio de Janeiro: Elsevier), 71–98. doi:10.1016/B978-85-352-6937-6.50012-4

Kucera, M. (2007). "Chapter Six Planktonic Foraminifera as Tracers of Past Oceanic Environments," in *Proxies in Late Cenozoic Paleoceanography of Developments in Marine Geology*. Editors C. Hillaire-Marcel, A. de Vernal, and H. Chamley (Amsterdam: Elsevier), 1, 213–262. doi:10.1016/s1572-5480(07)01011-1

Lantzsch, H., Hanebuth, T. J. J., Chiessi, C. M., Schwenk, T., and Violante, R. A. (2014). The High-Supply, Current-Dominated continental Margin of southeastern South America during the Late Quaternary. *Quat. Res.* 81 (2), 339–354. doi:10.1016/j.yqres.2014.01.003

Laskar, J., Robutel, P., Joutel, F., Gastineau, M., Correia, A. C. M., and Levrard, B. (2004). A Long-Term Numerical Solution for the Insolation Quantities of the Earth. *A&A* 428 (1), 261–285. doi:10.1051/0004-6361:20041335

Le, J., and Shackleton, N. J. (1992). Carbonate Dissolution Fluctuations in the Western Equatorial Pacific during the Late Quaternary. *Paleoceanography* 7, 21–42. doi:10.1029/91PA02854

Lessa, D. V., Venancio, I. M., dos Santos, T. P., Belem, A. L., Turcq, B. J., Sifeddine, A., et al. (2016). Holocene Oscillations of Southwest Atlantic Shelf Circulation Based on Planktonic Foraminifera from an Upwelling System (Off Cabo Frio, Southeastern Brazil). *The Holocene* 26 (8), 1175–1187. doi:10.1177/0959683616638433

Lippold, J., Gruetzner, J., Winter, D., Lahaye, Y., Mangini, A., and Christl, M. (2009). Does Sedimentary $^{231}Pa/^{230}Th$ from the Bermuda Rise Monitor Past Atlantic Meridional Overturning Circulation. *Geophysical Research Letters*. 36. L12601. doi:10.1029/2009GL038068

Locarnini, R. A., Mishonov, A. V., Antonov, J. I., Boyer, T. P., Garcia, H. E., Baranova, O. K., et al. (2013). *World Ocean Atlas*. Editor A. Mishonov 2013.

Lorius, C., Jouzel, J., Raynaud, D., Hansen, J., and Treut, H. L. (1990). The Ice-Core Record: Climate Sensitivity and Future Greenhouse Warming. *Nature* 347, 139–145. doi:10.1038/347139a0

Loubere, P. (1991). Deep-sea Benthic Foraminiferal Assemblage Response to a Surface Ocean Productivity Gradient: a Test. *Paleoceanography* 6, 193–204. doi:10.1029/90PA02612

Lund, D. C., Tessin, A. C., Hoffman, J. L., and Schmittner, A. (2015). Southwest Atlantic Water Mass Evolution during the Last Deglaciation. *Paleoceanography* 30 (5), 477–494. doi:10.1002/2014pa002657

Mackensen, A. (2008). On the Use of Benthic Foraminiferal $\delta^{13}C$ in Palaeoceanography: Constraints from Primary Proxy Relationships. *Geol. Soc. Lond. Spec. Publications* 303, 121–133. doi:10.1144/SP303.9

Mahiques, M. M., Fukumoto, M. M., Silveira, I. C. A., Figueira, R. C. L., Bícego, M. C., Lourenço, R. A., et al. (2007). Sedimentary Changes on the Southeastern Brazilian Upper Slope during the Last 35,000 Years. *Acad. Bras. Ciênc.* 79 (1), 171–181. doi:10.1590/S0001-37652007000100018

McManus, J. F., Francois, R., Gherardi, J.-M., Keigwin, L. D., and Brown-Leger, S. (2004). Collapse and Rapid Resumption of Atlantic Meridional Circulation Linked to Deglacial Climate Changes. *Nature* 428 (6985), 834–837. doi:10.1038/nature02494

Milliman, J. D., Troy, P. J., Balch, W. M., Adams, A. K., Li, Y.-H., and Mackenzie, F. T. (1999). Biologically Mediated Dissolution of Calcium Carbonate above the Chemical Lysocline? *Deep Sea Res. Part Oceanographic Res. Pap.* 46 (10), 1653–1669. doi:10.1016/s0967-0637(99)00034-5

Morard, R., Füllberg, A., Brummer, G. A., Greco, M., Jonkers, L., Wizemann, A., et al. (2019). Genetic and Morphological Divergence in the Warm-Water Planktonic Foraminifera Genus *Globigerinoides*. *PLoS One* 14 (12), e0225246–30. doi:10.1371/journal.pone.0225246

Nagai, R. H., Ferreira, P. A. L., Mulkherjee, S., Martins, M. V., Figueira, R. C. L., Sousa, S. H. M., et al. (2014). Hydrodynamic Controls on the Distribution of Surface Sediments from the Southeast South American continental Shelf between 23°S and 38°S. *Continental Shelf Res.* 89, 51–60. doi:10.1016/j.csr.2013.09.016

Naik, S. S., Godad, S. P., Naidu, P. D., Tiwari, M., and Paropkari, A. L. (2014). Early- to Late-Holocene Contrast in Productivity, OMZ Intensity and Calcite Dissolution in the Eastern Arabian Sea. *The Holocene* 24 (6), 749–755. doi:10.1177/0959683614526936

Nees, S., Armand, L., De Deckker, P., Labracherie, M., and Passlow, V. (1999). A Diatom and Benthic Foraminiferal Record from the South Tasman Rise (southeastern Indian Ocean): Implications for Palaeoceanographic Changes for the Last 200,000 Years. *Mar. Micropaleontology* 38 (1), 69–89. doi:10.1016/S0377-8398(99)00039-0

Pereira, L. S., Arz, H. W., Pätzold, J., and Portilho-Ramos, R. C. (2018). Productivity Evolution in the South Brazilian Bight during the Last 40,000 Years. *Paleoceanography and Paleoclimatology* 33, 1339–1356. doi:10.1029/2018pa003406

Peterson, R. G., and Stramma, L. (1991). Upper-level Circulation in the South Atlantic Ocean. *Prog. Oceanography* 26 (1), 1–73. doi:10.1016/0079-6611(91)90006810.1016/0079-6611(91)90006-8

Petit, J. R., Jouzel, J., Raynaud, D., Barkov, N. I., Barnola, J.-M., Basile, I., et al. (1999). Climate and Atmospheric History of the Past 420,000 Years from the Vostok Ice Core, Antarctica. *Nature* 399, 429–436. doi:10.1038/20859

Petró, S. M., and Burone, L. (2018). Changes in Water Masses in the Late Quaternary Recorded at Uruguayan Continental Slope (South Atlantic Ocean)/Mudanças Nas Massas De Água Durante O Quaternário Tardio Registadas No Talude Continental Uruguaio (Oceano Atlântico Sul). *J. Sed. Env.* 3 (4), 280–289. doi:10.12957/jse.201810.12957/jse.2018.39156

Petró, S. M., Costa, E. O., Pivel, M. A. G., and Coimbra, J. C. (2018a). Lysocline and CCD Fluctuations Record in Pelotas Basin during the Late Quaternary. *Anuário IGEO UFRJ* 41 (2), 710–719. doi:10.11137/201810.11137/2018_2_710_719

Petró, S. M., Pivel, M. A. G., and Coimbra, J. C. (2021). Evidence of Supra-lysoclinal Dissolution of Pelagic Calcium Carbonate in the Late Quaternary in the Western South Atlantic. *Mar. Micropaleontology* 166. doi:10.1016/j.marmicro.2021.102013

Petró, S. M., Pivel, M. A. G., and Coimbra, J. C. (2018b). Foraminiferal Solubility Rankings: a Contribution to the Search for Consensus. *J. Foraminiferal Res.* 48 (4), 301–313. doi:10.2113/gsjfr.48.4.301

Pimenta, F. M., Campos, E. J. D., Miller, J. L., and Piola, A. R. (2005). A Numerical Study of the Plata River Plume along the Southeastern South American Continental Shelf. *Braz. J. oceanography* 53 (3/4), 129–146. doi:10.1590/S1679-87592005000200004

Piola, A. R., Campos, E. J. D., Moller, O. O., Charo, M., and Martinez, C. (2000). Subtropical Shelf Front off Eastern South America. *J. Geophys. Res.* 105(C3) (726), 6565–6578. doi:10.1029/1999jc000300

Piola, A. R., and Matano, R. P. Ocean Currents: Atlantic Western Boundary|Brazil Current/Falkland (Malvinas) Current, in Encyclopedia of Ocean Sciences, (2017), pp. 422–430. doi:10.1016/B978-0-12-409548-9.10541-X

Piola, A. R., Matano, R. P., Palma, E. D., Möller, O. O., and Campos, E. J. D. (2005). The Influence of the Plata River Discharge on the Western South Atlantic Shelf. *Geophys. Res. Lett.* 32, L01603. doi:10.1029/2004GL021638

Portilho-Ramos, R. C., Cruz, A. P. S., Barbosa, C. F., Rathburn, A. E., Mulitza, S., Venancio, I. M., et al. (2018). Methane Release from the Southern Brazilian Margin during the Last Glacial. *Sci. Rep.* 8, 5948. doi:10.1038/s41598-018-24420-0

Portilho-Ramos, R. d. C., Ferreira, F., Calado, L., Frontalini, F., and de Toledo, M. B. (2015). Variability of the Upwelling System in the southeastern Brazilian Margin for the Last 110,000years. *Glob. Planet. Change* 135, 179–189. doi:10.1016/j.gloplacha.2015.11.003

Portilho-Ramos, R. d. C., Pinho, T. M. L., Chiessi, C. M., and Barbosa, C. F. (2019). Understanding the Mechanisms behind High Glacial Productivity in the Southern Brazilian Margin. *Clim. Past* 15 (3), 943–955. doi:10.5194/cp-15-943-2019

R Core Team. (2019). *R: A Language and Environment for Statistical Computing*. Vienna: Austria. http://www.R-project.org/.

Rasmussen, T. L., Thomsen, E., Troelstra, S. R., Kuijpers, A., and Prins, M. A. (2002). Millennial-scale Glacial Variability versus Holocene Stability: Changes in Planktic and Benthic Foraminifera Faunas and Ocean Circulation in the North Atlantic during the Last 60,000 Years. *Mar. Micropaleontology* 47 (1-2), 143–176. doi:10.1016/S0377-8398(02)001159

Ravello, A. C., and Hillaire-Marcel, C. (2007). "The Use of Oxygen and Carbon Isotopes of Foraminifera in Paleoceanography," in *Proxies in Late Cenozoic Paleoceanography*. Editors C. Hillaire-Marcel and A. De Vernal (Amsterdam: Developments in Marine Geology, Elsevier).

Reid, J. L., Nowlin, W. D., Jr., and Patzert, W. C. (1976). On the Characteristics and Circulation of the Southwestern Atlanitc Ocean. *J. Phys. oceanography* 7, 62–91. doi:10.1175/1520-0485(1977)007<0062OTCACO>2.0.CO;2

Rex, M. A., and Etter, R. J. (2010). *Deep-sea Biodiversity: Pattern and Scale*. Cambridge: Harvard University Press, 354

Rex, M., Etter, R., Morris, J., Crouse, J., McClain, C., Johnson, N., et al. (2006). Global Bathymetric Patterns of Standing Stock and Body Size in the Deep-Sea Benthos. *Mar. Ecol. Prog. Ser.* 317, 1–8. doi:10.3354/meps317001

Riebesell, U. (2004). Effects of CO2 Enrichment on Marine Phytoplankton. *J. Oceanography* 60, 719–729. doi:10.1007/s10872-004-5764-z

Rodrigues, A. R., Pivel, M. A. G., Schmitt, P., de Almeida, F. K., and Bonetti, C. (2018). Infaunal and Epifaunal Benthic Foraminifera Species as Proxies of Organic Matter Paleofluxes in the Pelotas Basin, South-Western Atlantic Ocean. *Mar. Micropaleontology* 144, 38–49. doi:10.1016/j.marmicro.2018.05.007

Rodrigues, L. F., Macario, K. D., Anjos, R. M., Ketzer, J. M. M., Maraschin, A. J., Augustin, A. H., et al. (2020). Origin and Alteration of Organic Matter in Hydrate-Bearing Sediments of the Rio Grande Cone, Brazil: Evidence from Biological, Physical, and Chemical Factors. *Radiocarbon*, 62, 197–206. doi:10.1017/RDC.2019.109

Schiebel, R. (2002). Planktic Foraminiferal Sedimentation and the marine Calcite Budget. *Glob. Biogeochem. Cycles* 16 (4), 1–21. doi:10.1029/2001GB001459

Schiebel, R., and Hemleben, C. (2017). *Planktic Foraminifers in the Modern Ocean, Pp. 358*. Berlin, Germany: Springer. doi:10.1007/978-3-662-50297-6

Schlitzer, R. (2020). Ocean Data View. Available at: https://odv.awi.de.

Schönfeld, J. (2012). History and Development of Methods in Recent Benthic Foraminiferal Studies. *J. Micropalaeontol.* 31, 53–72. doi:10.1144/0262-821X11-008

Shackleton, N. J. (2000). The 100,000-year Ice-Age Cycle Identified and Found to Lag Temperature, Carbon Dioxide, and Orbital Eccentricity. *Science* 289, 1897–1902. doi:10.1126/science.289.5486.1897

Shakun, J. D., Clark, P. U., He, F., Marcott, S. A., Mix, A. C., Liu, Z., et al. (2012). Global Warming Preceded by Increasing Carbon Dioxide Concentrations during the Last Deglaciation. *Nature* 484, 49–54. doi:10.1038/nature10915

Siccha, M., and Kucera, M. (2017). ForCenS, a Curated Database of Planktonic Foraminifera Census Counts in marine Surface Sediment Samples. *Sci. Data* 4, 170109. doi:10.1038/sdata.2017.109

Silveira, I. C. A. d., Schmidt, A. C. K., Campos, E. J. D., Godoi, S. S. d., and Ikeda, Y. (2000). A corrente Do Brasil ao Largo da Costa Leste Brasileira. *Rev. Bras. Oceanogr.* 48 (2), 171–183. doi:10.1590/S1413-77392000000200008

Smith, C. R., Berelson, W., Demaster, D. J., Dobbs, F. C., Hammond, D., Hoover, D. J., et al. (1997). Latitudinal Variations in Benthic Processes in the Abyssal Equatorial Pacific: Control by Biogenic Particle Flux. *Deep Sea Res. Part Topical Stud. Oceanography* 44 (9-10), 2295–2317. doi:10.1016/S09670645(97)00022-210.1016/s0967-0645(97)00022-2

Sortor, R. N., and Lund, D. C. (2011). No Evidence for a Deglacial Intermediate Water $\Delta^{14}C$ Anomaly in the SW Atlantic. *Earth Planet. Sci. Lett.* 310 (1–2), 65–72. doi:10.1016/j.epsl.2011.07.017

Sousa, S. H. M., de Godoi, S. S., Amaral, P. G. C., Vicente, T. M., Martins, M. V. A., Sorano, M. R. G. S., et al. (2014). Distribution of Living Planktonic Foraminifera in Relation to Oceanic Processes on the southeastern continental Brazilian Margin (23°S-25°S and 40°W-44°W). *Continental Shelf Res.* 89, 76–87. doi:10.1016/j.csr.2013.11.027

Souto, D. D., de Oliveira Lessa, D. V., Albuquerque, A. L. S., Sifeddine, A., Turcq, B. J., and Barbosa, C. F. (2011). Marine Sediments from southeastern Brazilian continental Shelf: A 1200year Record of Upwelling Productivity. *Palaeogeogr. Palaeoclimatol. Palaeoecol.* 299, 49–55. doi:10.1016/j.palaeo.2010.10.032

Stramma, L., and England, M. (1999). On the Water Masses and Mean Circulation of the South Atlantic Ocean. *J. Geophys. Res.* 104 (C9), 20863–20883. doi:10.1029/1999JC900139

Suárez-Ibarra, J. Y., Frozza, C. F., Petró, S. M., and Pivel, M. A. G. (2021). Fragment or Broken? Improving the Planktonic Foraminifera Fragmentation Assessment. *PALAIOS* 36, 165–172. doi:10.2110/palo.2020.062

Toledo, F. A. L., Cachao, M., Costa, K. B., and Pivel, M. A. G. (2007). Planktonic Foraminifera, Calcareous Nannoplankton and Ascidian Variations during the Last 25 Kyr in the Southwestern Atlantic: A Paleoproductivity Signature? *Mar. Micropaleontology* 64 (1-2), 67–79. doi:10.1016/j.marmicro.2007.03.001

Toledo, F., Costa, K. B., Pivel, M. A. G., and Campos, E. J. D. (2008). Tracing Past Circulation Changes in the Western South Atlantic Based on Planktonic Foraminifera. *Rbp* 11 (3), 169–178. doi:10.4072/rbp.2008.3.03

Viana, A. R. (2001). Seismic Expression of Shallow-To Deep-Water Contourites along the South-Eastern Brazilian Margin. *Mar. Geophys. Researches* 22, 509–521. doi:10.1023/A:1016307918182

Waelbroeck, C., Labeyrie, L., Michel, E., Duplessy, J. C., McManus, J. F., Lambeck, K., et al. (2002). Sea-level and Deep Water Temperature Changes Derived from Benthic Foraminifera Isotopic Records. *Quat. Sci. Rev.* 21, 295–305. doi:10.1016/S0277-3791(01)00101-9

Wefer, G., Berger, W. H., Bijma, J., and Fischer, G. (1999). "Clues to Ocean History: A Brief Overview of Proxies," in *Use of Proxies in Paleoceanography: Examples from the South Atlantic*. Editors G. Fischer and G. Wefer (Berlin Heidelberg: Springer-Verlag), 68. doi:10.1007/978-3-642-58646-0_1

Weinkauf, M. F. G., and Milker, Y. (2018). The Effect of Size Fraction in Analyses of Benthic Foraminiferal Assemblages: A Case Study Comparing Assemblages from the >125 and >150 μm Size Fractions. *Front. Earth Sci.* 6, 37. doi:10.3389/feart.2018.00037

Weinkauf, M. F. G., Moller, T., Koch, M. C., and Kučera, M. (2013). Calcification Intensity in Planktonic Foraminifera Reflects Ambient Conditions Irrespective of Environmental Stress. *Biogeosciences*, 10, 6639–6655. doi:10.5194/bg-10-6639-2013

Weschenfelder, J., Baitelli, R., Corrêa, I. C. S., Bortolin, E. C., and dos Santos, C. B. (2014). Quaternary Incised Valleys in Southern Brazil Coastal Zone. *J. South Am. Earth Sci.* 55, 83–93. doi:10.1016/j.jsames.2014.07.004

Wycech, J., Kelly, D. C., and Marcott, S. (2016). Effects of Seafloor Diagenesis on Planktic Foraminiferal Radiocarbon Ages. *Geology* 44 (7), 551–554. doi:10.1130/G37864.1

Yasuhara, M., Hunt, G., Cronin, T. M., Hokanishi, N., Kawahata, H., Tsujimoto, A., et al. (2012). Climatic Forcing of Quaternary Deep-Sea Benthic Communities in the North Pacific Ocean. *Paleobiology* 38 (1), 162–179. doi:10.1666/10068.1

Zamelczyk, K., Rasmussen, T. L., Husum, K., Haflidason, H., de Vernal, A., Ravna, E. K., et al. (2012). Paleoceanographic Changes and Calcium Carbonate Dissolution in the central Fram Strait during the Last 20 Ka. *Quat. Res.* 78, 405–416. doi:10.1016/j.yqres.2012.07.006

Zweng, M. M., Reagan, J. R., Antonov, J. I., Locarnini, R. A., Mishonov, A. V., Boyer, T. P., et al. (2013). *World Ocean Atlas.* Editor A. Mishonov Technical, 2013.

Conflict of Interest: The authors declare that the research was conducted in the absence of any commercial or financial relationships that could be construed as a potential conflict of interest.

Publisher's Note: All claims expressed in this article are solely those of the authors and do not necessarily represent those of their affiliated organizations, or those of the publisher, the editors and the reviewers. Any product that may be evaluated in this article, or claim that may be made by its manufacturer, is not guaranteed or endorsed by the publisher.